ELECTROCHEMICAL SYNTHESIS OF COPPER FILMS: NUCLEATION AND GROWTH ANALYSIS

A THESIS SUBMITTED IN PARTIAL FULFILLMENT OF THE
REQUIREMENTS FOR THE
DEGREE OF

BACHELOR OF TECHNOLOGY
in
METALLURGICAL AND MATERIALS ENGINEERING

by

NEHA DAS (107MM008)
SHIBA ALAM (107MM009)
SUBHASHREE P. KANHAR (107MM021)

DEPARTMENT OF METALLURGICAL AND MATERIALS ENGINEERING
NATIONAL INSTITUTE OF TECHNOLOGY
ROURKELA
2011

ELECTROCHEMICAL SYNTHESIS OF COPPER FILMS: NUCLEATION AND GROWTH ANALYSIS

A THESIS SUBMITTED IN PARTIAL FULFILLMENT OF THE
REQUIREMENTS FOR THE
DEGREE OF

BACHELOR OF TECHNOLOGY
in
METALLURGICAL AND MATERIALS ENGINEERING

by

NEHA DAS (107MM008)
SHIBA ALAM (107MM009)
SUBHASHREE P. KANHAR (107MM021)

UNDER THE GUIDANCE OF

PROF. ARCHANA MALLIK

DEPARTMENT OF METALLURGICAL AND MATERIALS ENGINEERING
NATIONAL INSTITUTE OF TECHNOLOGY
ROURKELA
2011

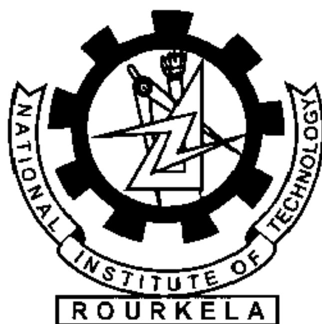

National Institute of Technology Rourkela

CERTIFICATE

This is to certify that the thesis entitled, "**Electrochemical Synthesis of Copper Films: Nucleation and Growth Analysis"** submitted by **Neha Das (107MM0008)**, **Shiba Alam** (**107MM009**) and **Subhashree Priyadarshini Kanhar** (**107MM021**) in partial fulfillment of the requirements for the award of **Bachelor of Technology Degree** in **Metallurgical and Materials Engineering** at National Institute of Technology, Rourkela is an authentic work carried out by them under my supervision and guidance.

To the best of my knowledge, the matter embodied in the thesis has not been submitted to any other University/Institute for the award of any Degree or Diploma.

Date:

Dr. Archana Mallik
Dept. of Metallurgical and Materials Engineering
National Institute of Technology
Rourkela-769008

Acknowledgement

We take this opportunity to express our deep regards and sincere gratitude to our guide **Dr. Archana Mallik** for her constant guidance and concern during the execution of the project. She will always be a constant source of inspiration for us. We also express our sincere gratitude to, **Dr. B.B. Verma**, HOD, Metallurgical and Materials Engineering for providing valuable departmental facilities. We extend our thanks to **Dr. B.C Ray** for his concern and encouragement. We are also thankful to technical assistants, **R. Pattanaik** Sir and **U. K. Sahu** Sir, of Department of Metallurgical and Materials Engineering, NIT Rourkela, for constant practical assistance and help whenever required. We are grateful to **Ms. Arpita Das** for sparing her valuable time in clearing our doubts and conducting the experiments successfully. We would also like to thank all the staff members of **MME Dept., NITR** and everyone who in some way or the other has provided us valuable guidance, suggestion and help for this project.

Place: Rourkela

Date:

Neha Das (107MM008)

Shiba Alam (107MM009)

Subhashree Priyadarshini Kanhar (107MM021)

Abstract

Thins films are deposited on bulk materials to attain properties which are superior to the parent substrates. In this project Cu thin films have been synthesized on graphite substrate using the electrodeposition technique. Deposition occurs by a process of nucleation and growth. The mechanisms related to the initial stages of the nucleation and growth of Cu thin films on the rough face side of graphite have been studied as a function of temperature, Cu concentration and acid concentration. The analysis of the corresponding potentiostatic *j*/t transients suggests that the deposition takes place according to instantaneous nucleation 3D diffusion controlled growth, giving account for the formation of hemispherical nuclei. The extent of nucleation was found to be increased with decreasing temperatures and increasing metal ion and acid concentration, with spherical copper deposition. Ex situ SEM images and XRD analysis of the surface seem to support these assumptions.

Keywords: Electrodeposition, Potentiostatic, Nucleation and Growth, Temperature, Electrolyte composition, Copper.

Contents

Contents	**Page No.**
Certificate	i
Acknowledgement	ii
Abstract	iii
List of figures	vi-vii
List of tables	viii
1. CHAPTER I: Introduction	**1-3**
1.1.Background	1
1.2.Objectives	2
1.3.Structure of the thesis	2
2. CHAPTER II: Literature review	**4-19**
2.1.Thin films	4
2.2.Synthesis of thin films	5
2.2.1.Physical deposition	5
2.2.2.Chemical deposition	7
2.2.3.Other deposition processes	8
2.3.Electrodeposition	9
2.4.Nucleation and growth mechanism	10
2.5.Factors affecting nucleation and growth of thin films during electrodeposition	14

2.5.1.Effect of temperature 14

2.5.2.Effect of acid concentration 15

2.5.3.Effect of Copper concentration 15

2.6.Nucleation and growth analysis 16

2.6.1.Cyclic Voltammetry 16

2.6.2.Chronoamperometry 18

3. CHAPTER III: Experimental details 20-24

3.1.Chemicals and substrates 20

3.2.Substrate preparation 20

3.3.Electrolytic bath preparation 20

3.4.Electrochemical cell and instrumentation 22

3.5.Cyclic Voltammetry 23

3.6.Chronoamperometry 23

3.7.Characterization technique 23

4. CHAPTER IV: Results and discussion 25-42

4.1.Voltammetric study 25

4.2.Chronoamperometric study 27

4.3.Mathematical modeling 29

4.3.1.2D Model 30

4.3.2.3D Model 33

4.4.Phase and structural analysis 37

5. CHAPTER V: Conclusion 43

6. REFERENCES 44-47

List of figures

Figure No.	Caption	Page No.
1	Initial stages of nucleation at the region near the interface.	10
2	Changes in surface and volume free energies with size nuclei.	12
3	The Nucleation rate I and the growth rate U as a function of temperature.	13
4	Variables affecting electrochemical phase formation.	14
5	(a) A cyclic voltammetry potential wave from with switching potentials and (b) The expected response of a reversible redox couple during a single potential cycle.	17
6	A typical Chronoamperogram showing double layer charging	18
7	Schematic diagram of the Electrochemical cell used	22
8	A set of cyclic voltammograms for the graphite electrode in $CuSO_4$ bath ($10gl^{-1}$ Cu^{2+} and $60gl^{-1}$ H_2SO_4) at a scan rate of 10 mV s^{-1} for different temperatures indicated.	26
9	Current transients obtained for (a) a particular temperature 15°C at different potentials and (b) at different temperatures for a particular potential – 0.40 V	27
10	Current transients obtained for (a) a particular copper concentration $15gl^{-1}$ at different potentials (b) at – 0.45 V for copper concentrations of 10 gl^{-1}, 15 gl^{-1}, and 20 gl^{-1}	28
11	Current transients obtained for (a) a particular acid concentration of $40gl^{-1}$ at different potentials (b) – 0.40 V at acid concentrations of $20gl^{-1}$, 30 gl^{-1}, and 40 $gl^{-1}$and 50 gl^{-1}	29
12	Dimensionless plots according to the equations (1) and (2) for two dimensional growth of copper deposits at (a) 5°C (b) 10°C (c) 15°C	31

	(d) 20°C (e) 25°C for a potential of – 0.45 V	
13	Dimensionless plots according to equations (1) and (2) for two dimensional growth of copper deposits at Copper concentrations of (a) 10gpl (b) 15 gpl and (c) 20gpl at a potential of –0.35 V	32
14	Dimensionless plots according to the equations (1) and (2) for two dimensional growth of copper deposits at acid concentrations of (a) 20gpl (b) 30 gpl and (c) 40 gpl at a potential of –0.25 V	33
15	Dimensionless plots according to the equations (3) and (4) for three dimensional growth of copper deposits at (a) 5°C (b) 10°C (c) 15°C (d) 20°C (e) 25°C	34
16	Dimensionless plots according to the equations (3) and (4) for three dimensional growth of copper deposits at 20 °C for increasing potentials of (a)– 0.20 V, (b)– 0.25 V, (c)– 0.30 V,(d) – 0.35 V, (e)– 0.40 V and (f)– 0.45 V	35
17	Dimensionless plots according to the equations (3) and (4) for three dimensional growth of copper deposits at varying copper concentrations of (a)10 gl^{-1} (b)15 gl^{-1} (c) 20 gl^{-1}	36
18	Dimensionless plots according to the equations (3) and (4) for three dimensional growth of copper deposits at varying acid concentrations of (a)20 gl^{-1} (b)30 gl^{-1} (c) 40 gl^{-1}	37
19	SEM images of copper deposits at (a)5°C, (b)10°C, (c)15°C, (d)20°C and (e)25°C	38
20	SEM images of copper deposits at varying copper concentrations of (a)10 gl^{-1}, (b) 15gl^{-1} (c) 20 gl^{-1}	39
21	SEM images of copper deposits at varying acid concentrations(a) 20 gl^{-1}, (b) 30gl^{-1}, (c) 40 gl^{-1} and (d) 50 gl^{-1}	40
22	XRD patterns for the Cu films deposited at varying (a) temperatures (b) copper concentrations and (c) Acid concentrations	41

List of tables

Table No.	Caption	Page No.
1	Electrolytic bath composition	21
2	Parameters obtained from the cyclic voltammograms of the graphite electrode in $CuSO_4$ solution at different temperatures (a) 5°C (b) 10°C (c) 15°C (d) 20°C and (e) 25°C	25
3	Crystallite size and lattice strain obtained by varying different parameters	42

CHAPTER –I

Introduction

1. Introduction

1.1. Background

Thin films are materials with a very high surface to volume ratio, and a thickness equal to less than 1 μm. Thin films behave differently from bulk materials of the same chemical composition. These differences arise because of various factors like smaller size of the crystallites and many crystallographic defects such as dislocations, vacancies, stacking faults, grain boundaries and twins which are present in different degrees and orders. It has been found that most of the thin film properties (mechanical, electrical, optical and magnetic) are far more superior to the bulk properties and can replace it when the latter fail to meet an application requirement [1]. But inspite of their upgrade properties, their reliability is affected by the growth of the films during the service and operation of the device. Grain growth of the films can cause a decrease in resistivity, hardness and the strength of the material. So in order to obtain thin films with desired structure and stoichiometry, it is very important to study their deposition structure, growth and properties in a detailed manner and then be able to predict the optimal conditions for a particular deposition technique [2].

There are different synthesis routes to develop these thin films such as physical vapour deposition (PVD), chemical vapour deposition (CVD), molecular beam epitaxy (MBE), spin coating and electrodeposition. In our project we have followed the electrochemistry route. Electrodeposition technique offers various advantages like low processing temperatures, control of film thickness, easy deposition onto complex shapes, low capital investment and the

production of non-equilibrium materials which cannot be accessed by other traditional processes. We have deposited copper thin films by the electrodeposition process. The deposited film depends on various parameters like temperature, concentration of electrolyte etc. An attempt has been made to study the effect of these parameters on the nucleation and growth behaviour, by electrochemical techniques like cyclic voltammetry and chronoamperometry. Microstructural analysis was done using SEM and structural and phase analysis was carries out using XRD. The results obtained show that nucleation is favoured as temperature is decreased.

1.2. Objectives

The objectives to be achieved in the project are:

- To study the effects of varying temperature and electrolyte concentration on morphology of copper deposits while restricting the study to the nucleation and growth stages only.
- To carry out the in process analysis of the copper deposition followed by mathematical modeling.
- To conduct post synthesis analysis of the copper deposits by SEM and XRD.

1.3. Structure of the thesis

This thesis has been divided into 5 chapters.

In **chapter 2** a brief idea about thin films and their synthesis has been given with special emphasis on the electrodeposition route of synthesis. The various electrochemical techniques and mathematical models found in literature which we have used in our project have been discussed here. In **chapter 3** the experimental details have been described: electrochemical cell arrangement, X Ray Diffraction and Scanning Electron Microscopy. **Chapter 4** includes the results of cyclic voltammetry, chronoamperometry and structural analysis techniques to study the effect of the three parameters namely temperature, acid concentration and Copper concentration.

Chapter 5 summarizes the results obtained from experimentation and finally a list of references which have been referred for the project has been given at the end of the thesis.

CHAPTER –II
Literature review

2. Literature Review

2.1. Thin films

A material is classified into a thin film when it has a thickness ranging from fractions of a nanometer to less than one micrometer. Materials with a thickness greater than a micrometer are classified as coatings. Coatings are mostly used for structural applications such as protective covering on cutting tools to improve their wear resistance and hardness. Thin films, however, have both structural and functional applications. They not just improve the endurance of the surface but the overall life of the component. Because of their upgraded optical, electrical, magnetic, chemical and mechanical properties they find use in reflective and anti-reflective coatings [3], compact discs, sensors, semiconductor devices etc [4].

Mechanical properties of thin films often differ from those of their bulk counterparts. This is because of the very small size of thin films (in the nano range) and the fact that these films are attached to a substrate. Thin films can support very high residual stresses. This residual stress can be relieved later during processing or in the actual device operation through plastic deformation, thin film fracture, or interfacial delamination [5]. The level of the intrinsic stress is comparable with the yield strength of many bulk materials and thus influences the physical and mechanical stability and the properties of the films. The presence of large number of defects and free surfaces hinder the generation and movement of dislocations in a film. This results in the enhancement of the tensile strength of films up to 200 times the value in the corresponding bulk

material. Flow stresses of thin metal films deposited on rigid substrates are also found to be significantly higher than those observed in the corresponding bulk materials.

2.2. Synthesis of thin films

Thin Film synthesis techniques used in the laboratory are based on physical or chemical vapor deposition. In both cases, the techniques are based on the formation of vapor of the material to be deposited, so that the vapor is condensed on the substrate surface as a thin film. Usually the process must be performed in vacuum or in controlled atmosphere, to avoid interaction between vapor and air.

2.2.1.Physical deposition

Physical deposition makes use of a mechanical or thermodynamic means to produce a thin film of solid. Formation of frost is a good example. Since most engineering materials are held together by relatively high energies, and chemical reactions are not used to store these energies, commercial physical deposition systems tend to require a low-pressure vapor environment to function properly; most can be classified as Physical vapor deposition or PVD [6].

The material which has to be deposited is kept in an energetic, entropic environment, so that they can escape easily from the surface. As these particles arrive, a cooler surface which is placed in front of the source draws energy from them, allowing the formation of a solid layer over itself. In order to allow the particles to travel freely (increase mean free path), the system is kept in a very low pressure or vacuum deposition chamber. Films deposited by physical vapour deposition method are commonly directional, rather than conformal, as particles tend to follow a straight line.

Physical deposition includes:

- A **thermal evaporator** makes use of an electric resistance heater to melt the material and increase its vapor pressure to a useful range. This is carried out in high vacuum, so that the vapor can reach the substrate without interacting with or scattering against other gaseous atoms present in the chamber, and reduce the inclusion of impurities from the residual gas in the vacuum chamber. Obviously, only materials with a much higher vapor pressure than the heating element can be deposited without contamination of the film. Molecular beam epitaxy is a particular form of thermal evaporation.
- An **electron beam evaporator** fires a high-energy beam from an electron gun to boil a small spot of material; since the heating is not uniform, materials having lower vapor pressure can be deposited. The beam is generally bent through an angle of 270° so as to ensure that the gun filament is not directly exposed to the evaporant flux. Typical deposition rates for electron beam evaporation lie between 1 to 10 nanometers per second.
- **Sputtering** relies on a plasma (usually a noble gas, such as Argon) to knock out material from a "target" a few atoms at a time. The target can be kept at a comparatively low temperature, since the process does not involve evaporation. This makes sputtering one of the most flexible techniques for deposition. It is specifically useful for compounds or mixtures, where have components that evaporate at different rates. Sputtering step coverage is more or less conformal.
- **Pulsed laser deposition** systems work on the basis of an ablation process. Pulses of focused laser light are used to vaporize the surface of the target material and convert it to plasma. This plasma reverts to a gas before it reaches the substrate.

- **Cathodic Arc Deposition** or Arc-PVD is a kind of ion beam deposition where an electrical arc that is created blasts ions from the cathode. The arc has an extremely high power density resulting in a high level of ionization (30-100%), multiply charged ions, neutral particles, clusters and macro-particles (droplets). If a reactive gas is introduced during the evaporation process, dissociation, ionization and excitation can occur during interaction with the ion flux and a compound film will be deposited.

2.2.2. Chemical deposition

In this process, a fluid precursor undergoes a chemical reaction at a solid surface, forming a solid layer. A perfect example would be the formation of soot on the surface of a cool object when it is placed inside a flame. Since the fluid surrounds the solid object, deposition happens uniformly on every surface, rather than any particular direction. Thin films formed by chemical deposition techniques tend to be conformal, rather than directional.

Chemical deposition can be further categorized on the basis of phase of the precursor:

- **Plating** relies on liquid precursors, which are often a solution of water containing a salt of the metal which has to be deposited. Some plating processes are driven by reagents in the solution (usually for noble metals), but by far the most commercially important process is electroplating. It was not commonly used in semiconductor processing for many years, but has seen resurgence with more widespread use of Chemical-mechanical polishing techniques.
- **Chemical Solution Deposition** (CSD) uses a liquid precursor, usually a solution containing organometallic powders dissolved in an organic solvent. This process is inexpensive and simple and can produce stoichiometrically accurate crystalline phases.

- **Chemical vapor deposition** (CVD) commonly uses a gas-phase precursor, like a halide or hydride of the element which is to be deposited. An organometallic gas is used in the case of MOCVD. Commercial techniques generally use very low pressures of precursor gas.
- **Plasma enhanced CVD** makes use of an ionized vapor, or plasma, as the precursor. PECVD relies on electromagnetic means (electric current, microwave excitation), rather than a chemical reaction, for the production of a plasma.

2.2.3. Other deposition processes

There are some methods which rely on a mixture of both chemical and physical means:

- **Molecular beam epitaxy** (MBE), slow streams of an element is directed at the substrate, so that deposition occurs one atomic layer at a time. Compounds (like Gallium Arsenide) are usually deposited by repeated application of a layer of one element (i.e., Ga), then a layer of the other (i.e., As), making the process both chemical, as well as physical. The beam of material can be generated by either physical means (that is, by a furnace) or by a chemical reaction (chemical beam epitaxy).
- **Spin coating** is a process of application of uniform thin films to flat substrates. Excess amount of a solution is kept on top of a substrate, which is then rotated at high speed so that the fluid spreads by centrifugal force. The machine used for spin coating is called a spin coater, or spinner. Rotation is continued until the film has achieved desired thickness. The applied solvent being volatile evaporates simultaneously during the process. The higher the angular speed of spinning, the thinner the film. Concentration of the solution and the solvent also affect the thickness of the film. Spin coating is extensively used in micro fabrication, where it can be used to create thin films with thicknesses below 10 nm. It is used intensively in photolithography, to

deposit layers of photoresist about 1 micrometer thick. Photoresist is typically spun at 20 to 80 Hz for 30 to 60 seconds [7].

2.3. Electrodeposition

Electrochemical deposition involves the synthesis of solid films from dissolved species by changing their oxidation states using electricity. Pure metals as well as compounds like oxides and phosphides can be easily fabricated by electrochemical deposition. Some of the important applications familiar in the electronics industry are the electrodeposition of copper interconnects in integrated circuits and the deposition of thin film magnetic materials, e.g. CoNiFe alloys [8].

It has also been applied in nanotechnology since it can be used to fill three-dimensional features at room temperature with good control of thickness and morphology. Electrodeposition has various advantages over other processing techniques.

It is a cost-effective method for preparation of materials (metals, alloys, compositionally modulated alloys and composites) in the form coatings or as freestanding objects even in complex shapes (foils, wires, electroforms). Very low processing temperatures can be attained easily. Low temperature minimizes interdiffusion or chemical reaction. Deposition can be carried out in a selected specific area and thickness of the deposit can be controlled accurately by monitoring the consumed charge. Deposition rates are in the order of several tens of microns per hour [9, 10]. Electrodeposition is a very convenient technique for producing thin multilayered materials. Coherence and uniformity in layer thickness obtained in coatings by electrodeposition can match those of composition-modulated alloys produced by vacuum evaporation or sputter deposition.

All the electrochemical reactions take place at the interface between the electrode and the electrolyte and the driving force of these reactions is the electrical and chemical potentials

developed in the electrolyte. Electrodeposition occurs in a very thin region in front of the electrode. The ions have to pass through an electrical double layer present on the cathode surface. This double layer acts like a parallel plate condenser with one plate being the metal surface with excess charge and the other plate is formed by the solvated ions. Most anions however give away part of that solvation shell when entering the double layer to form a chemical bond with the electrode surface.

2.4. Nucleation and growth mechanism

Nucleation and growth are one of the two major mechanisms for the formation of thin films during electrodeposition.

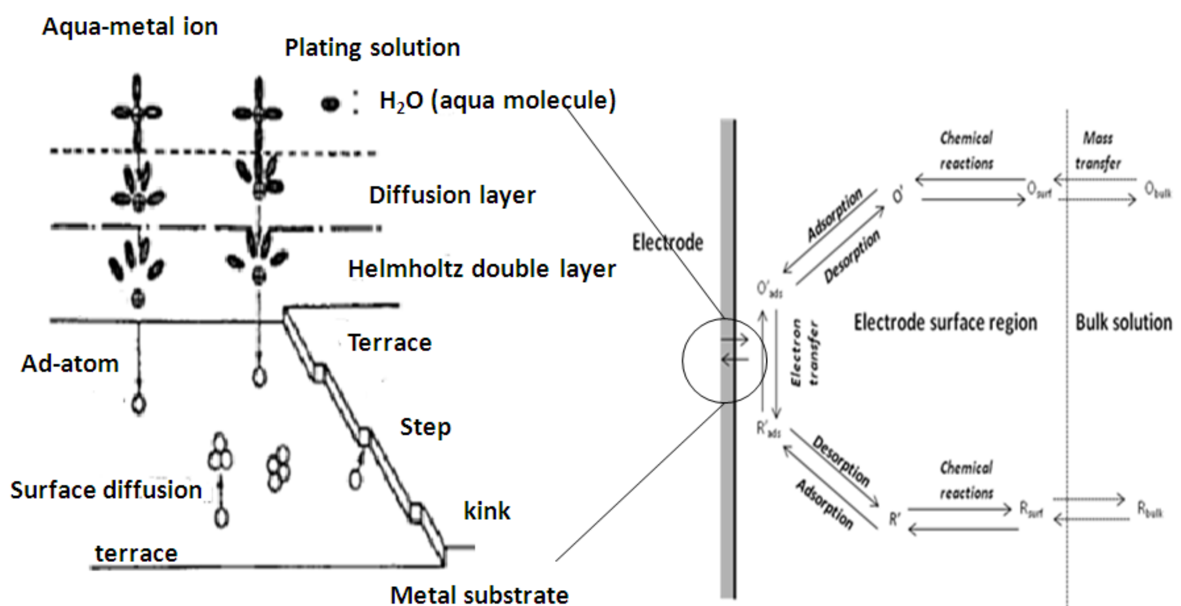

Fig.1. Initial stages of nucleation at the region near the interface.

Metal ions are present in a hydrated state in the bulk electrolyte. When a potential is applied they move towards the cathode due to the potential gradient. Then these ions pass through a diffusion layer and an electrical double layer and the process they get stripped off from the hydrated complex and become bare metal ions. The bare metal ions then get discharged by combining

with electrons on the surface of the cathode and become neutral atoms. These atoms then start migrating over the substrate until they get adsorbed at active sites. Kinks and steps present on the surface act as active sites for adsorption (Fig.1.). Successive adsorption of atoms at such sites results in continuous spreading of the mono atomic layer over the substrate surface [11, 12].

The adsorbed species are not in thermal equilibrium with the substrate initially and move over the substrate surface. And in this process they interact with themselves forming bigger clusters. The clusters are thermodynamically unstable and get desorbed with time. But if the cluster collides with other such adsorbed species before getting desorbed, it starts growing in size. After a certain critical size is reached, the cluster overcomes the nucleation barrier and becomes thermodynamically stable. The critical nuclei grow in number as well as in size until a saturation nucleation density is reached. Next stage is coalescence in which the small nuclei clusters coalesce with each other in order to reduce the surface. This tendency of forming bigger clusters is known as agglomeration and it is enhanced by increasing surface mobility of the adsorbed species. When larger islands grow they leave certain portions of uncovered substrate in the form of channels and holes which are then later on filled up forming a continuous film.

Nucleation is the process in which a new phase is generated from an old phase when its free energy becomes higher than that of the emerging new phase. The transformation from old phase to new phase occurs only when the nuclei overcome a free energy barrier. This can be understood by considering the free energy changes associated with the formation of a nucleus (Fig.2.).

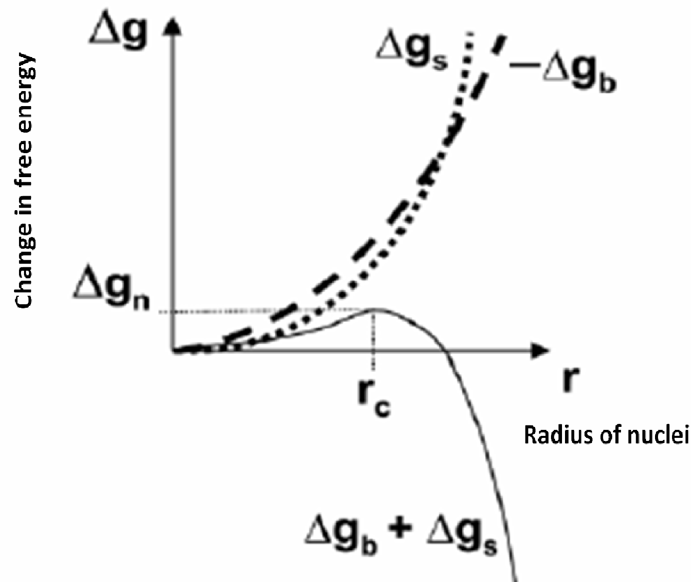

Fig.2. Changes in surface and volume free energies with size nuclei.

Molecules present at the surface of the nuclei are less well bound to their neighbours than those molecules which are present at the interior. So, their contribution to the free energy of the new phase is greater. The difference between the energies of the surface molecules and those that are present in the bulk is termed as surface free energy. When size of the nucleus is small there is more number of molecules at the surface and the nucleus is unstable. So addition of more molecules increases the energy of the system, and the nucleus dissolves. But once the nucleus size is large enough, the drop in the free energy of the system due to the formation of the bulk phase is much larger than the surface free energy resulting in an overall decrease in the free energy of the system. This intermediate size at which the free energy of the system is decreased whether the nucleus grows or dissolves is known as the critical size. The probability of nucleation thus is affected by the size of the critical nucleus which a function of the interfacial energy. The smaller the interfacial energy, the smaller is the critical size required for nucleation and thus formation of new phase is easier. The probability of nucleation can hence be

manipulated by varying the solution composition or supersaturation [13]. The figure below shows the change in the overall free energy change associated with the formation of the new phase.

Growth is defined as the increase in size of the particle beyond the critical size. The relative rates of nucleation and growth decide the size of the grain. Large number of grains is obtained if nucleation rate is high. High nucleation rate combined with a low growth rate results in fine grained structure [14, 15].

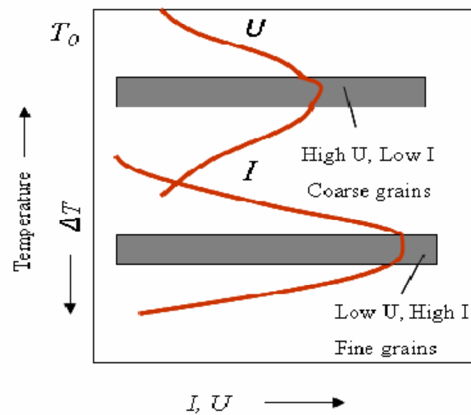

Fig.3. Nucleation rate I and the growth rate U as a function of temperature.

Furthermore nucleation and growth mechanism has also been classified into interfacial (or charge) controlled and diffusion controlled. In charge control the growth rate is limited by the rapidity with which the ions are incorporated into the new phase while in diffusion control the growth is limited by the rate at which the material is transported through the solution to the electrode surface. The former is favored by high concentrations and low deposition overpotentials and the latter is favored by low concentrations and high overpotentials [30].

2.5. Factors affecting nucleation and growth of thin films during electrodeposition

There are various factors which affect the nucleation and growth of deposits bath temperature, composition, agitation of the electrolyte etc. These have been summarized in the figure below (Fig.4.).

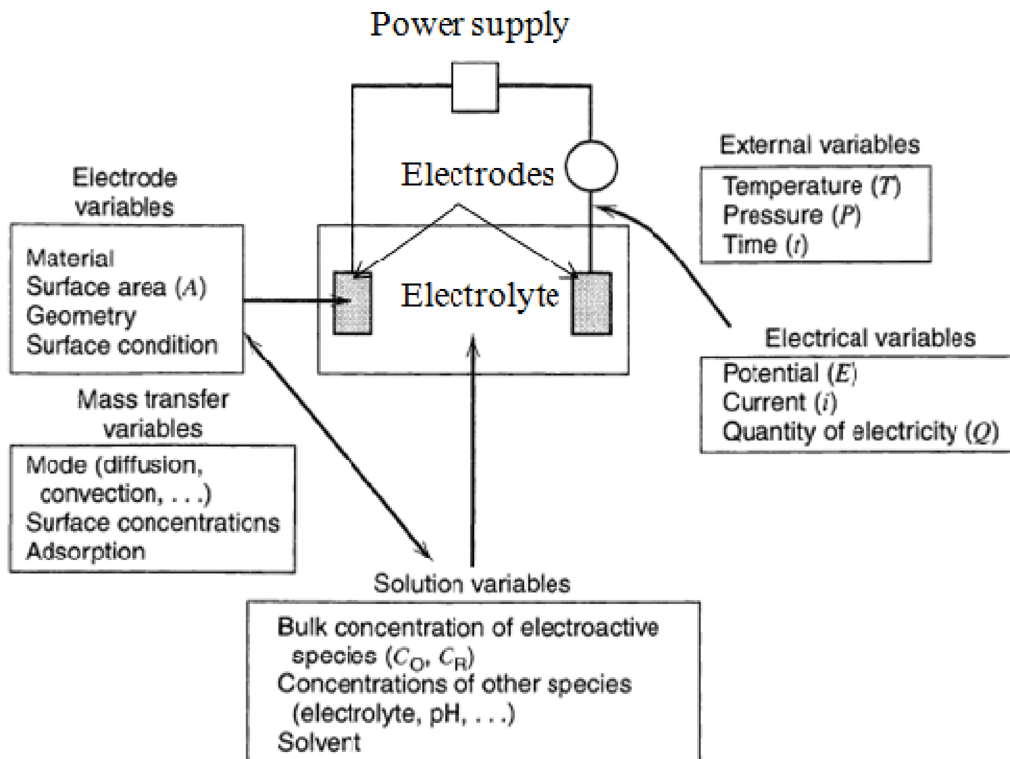

Fig.4. Variables affecting electrochemical phase formation

2.5.1. Effect of temperature

The velocity or diffusion of metal ions in the electrolyte increases with increase in temperature ($D = D_0\, e^{\frac{-Q}{RT}}$). An increase in temperature causes an increase in the ion supply towards the cathode thereby decreasing the cathodic overpotentials. This increases the energy of nucleation. An increased energy for nucleation implies decreased rate of nuclei formation and preferred growth of existing nuclei resulting in the formation of large grains [16 - 19].

2.5.2. Effect of acid concentration.

Results obtained by studying the variation in the surface morphology with acid concentration reveal that the formation of smooth bright deposits is favored at lower concentrations. However medium concentration values tend to enhance the rate of nucleation. Hardness value also tends to decline when the concentration is increased [20]. As the acid concentration is increased the electrode potential shifts towards more positive values within the cathodic range and more negative within the anodic range. The cathodic efficiency decreases with the increasing alkalinity of the solution beyond the 8.5 value [21]. Open circuit potential of the metal does not change with time; its value is dependent on the solution concentration value, i.e. concentration of $H+$ ion, and becomes more negative as the concentration increases in an acidic solution. Decreasing concentration of acid in the electrolyte led to the increase of hydrogen evolution reaction and hydrogen bubbles which cling to the surface and decrease the effective surface area of the metal reduction reaction. The crystallinity and grain size in the deposits decreased with the decrease of bulk concentration due to a high polarization [22].

2.5.3. Effect of Copper concentration

As the concentration of Copper increases in the bath the rate of nucleation and growth is found to be higher and the formation of thin films becomes easier. With higher current density the deposits which are formed are coarse in nature (spongy and dark). Studies also suggest that the increased concentration of copper in the electrolyte bath favors the formation of fresh nuclei.

Certain experiments, however, indicate that the rate of formation of nuclei is actually decreased by increasing concentration, but the improvement in the deposit is due to an increase in the rate of growth of crystals over the cathode surface [23]. The electrodeposition is mostly used to obtain metallic films of adequate thickness, structure and adhesion [24]. The nature of metal

surface influences the nature of thin deposit [25], and the properties of thicker deposits are mainly influenced by the bath condition [26].

2.6. Nucleation and growth analysis

The nucleation and growth analysis was carried out using electrochemical techniques like cyclic voltammetry and chronoamperometry and then modeling was done using various mathematical models.

2.6.1. Cyclic Voltammetry

Cyclic voltammetry is a very versatile electrochemical technique which allows probing the mechanics of redox and transport properties of a system in solution. A three electrode arrangement is used in which the potential relative to some *reference* electrode is scanned at a *working* electrode while the resulting current flowing through a *counter* (or *auxiliary*) electrode is monitored in a quiescent solution. The technique makes a quick search of redox couples present in a system and once located; a couple may be characterized by more careful analysis of the cyclic voltammogram. Usually the potential is scanned back and forth linearly with time between two extreme values – the switching potentials using triangular potential waveform (see Fig.5.). The scan shown in the figure starts at a slightly negative potential, *(A)* up to some positive switching value, *(D)* at which the scan is reversed back to the starting potential. The current is first observed to peak at *Epa* (with value *ipa*) indicating that an oxidation is taking place and then drops due to depletion of the reducing species from the diffusion layer. During the return scan the processes are reversed (reduction is now occurring) and a peak current is observed at *Epc* (corresponding value, *ipc*) [2].

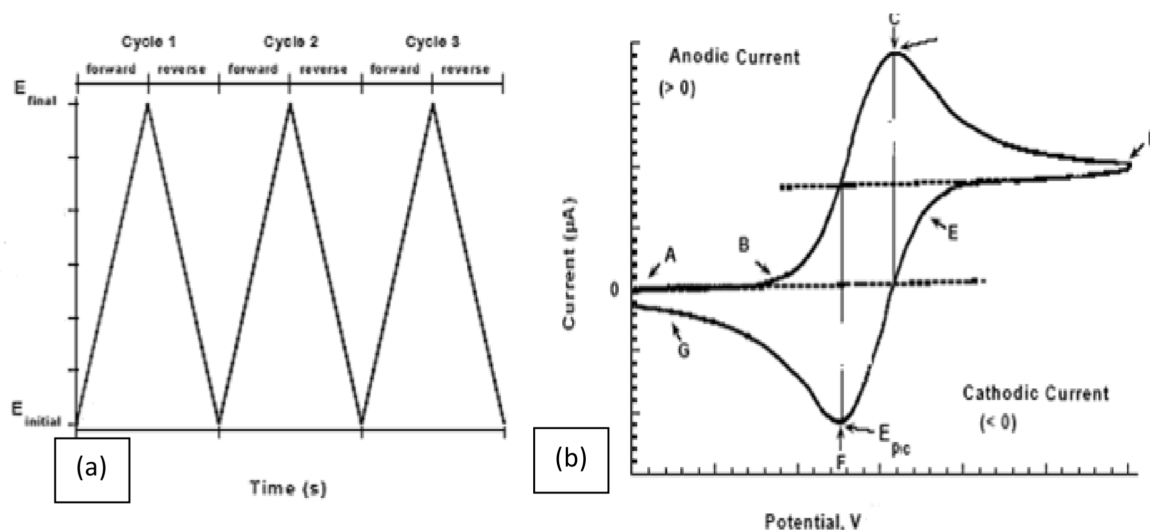

Fig.5. ***(a) A cyclic voltammetry potential wave from with switching potentials and (b) The expected response of a reversible redox couple during a single potential cycle***

The magnitude of the observed faradic current can provide information on the overall rate of the many processes occurring at the working electrode surface. As is the case for any multi–step process, the overall rate is determined by the slowest step. In general, the electrode reaction rate is governed by the rates of processes such as:

1) Mass transfer (e.g., of O from the bulk solution to the electrode surface).

2) Electron transfer at the electrode surface.

3) Chemical reactions preceding or following the electron transfer. These might be homogeneous processes (e.g., protonation or dimerization) or heterogeneous ones (e.g., catalytic decomposition) on the electrode surface.

4) Other surface reactions, such as adsorption, desorption, or crystallization (electrodeposition)

2.6.2. Chronoamperometry

Potentiostatic transients or chronoamperograms are used for the evaluation of induction times, nucleation rate constants, nuclear number densities and the mode of nuclei appearance. A typical current-time transient for nucleation with overlapping is shown in the figure below (Fig.6.).

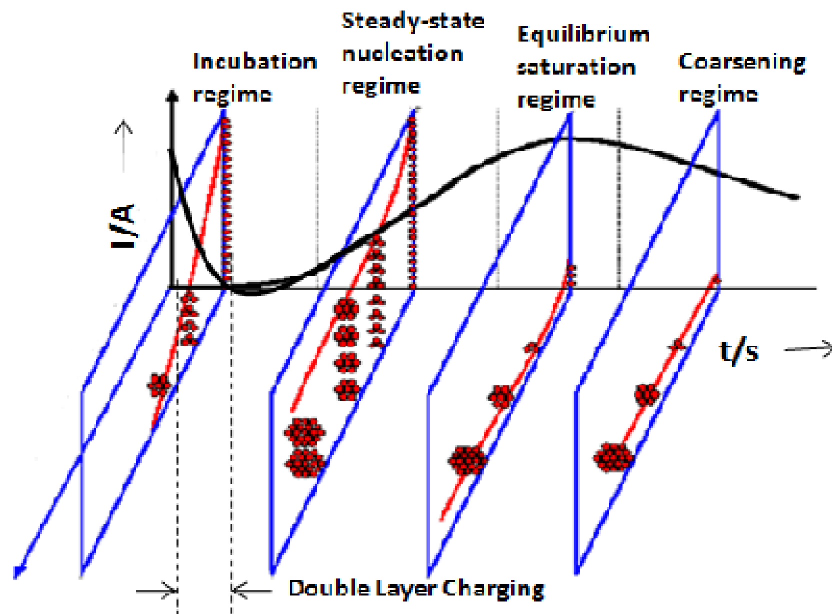

Fig.6. A typical Chronoamperogram showing double layer charging

The current transient shows a falling current section, a rising section and again a falling section corresponding to double layer charging, nuclei appearance on the substrate and the subsequent growth of electro active area as established nuclei grow. Fleischmann and Thirsk, and Pangarov worked on 'constant overvoltage' for studying the nucleation and growth of electrodeposited materials [27, 28]. The current-time transients they recorded showed maxima [29], which were followed, by approximately exponential decay. This suggested that the nuclei were formed according to the equation:

$$\frac{dN}{dt} = ANo\, e^{(-At)} \qquad (2.1)$$

Where, t is the time since the potential was applied; N is the number of nuclei, N_0 is the saturation nucleus density (number of active sites) A is the nucleation rate constant (a potential dependent constant with units of nuclei s^{-1}). This nucleation rate law is of great significance and it is assumed as a basis for an entire family of more sophisticated models developed for the analysis of the process.

CHAPTER –III

Experimental details

3. Experimental details

3.1. Chemicals and substrates

Copper sulfate (Cu_2SO_4. $5H_2O$) and sulfuric acid (H_2SO_4) of analytical grade were obtained and used as received without further purification. Aqueous solution was prepared from doubly distilled water. Graphite sheets (working electrode) were from Asbury Ltd. USA. All other chemical were used as received.

3.2. Substrate preparation

Graphite samples were cut from a sheet of graphite (10 cm X 10 cm) using a hacksaw. The samples were cleaned in an ultrasonic cleaner for 20 minutes using acetone and water. The samples were then taken out, polished and dried. An area of 0.25 cm^2 was marked on the graphite samples by carefully covering the rest part with non-conducting tape

3.3. Electrolytic bath preparation

For experiments involving temperature variation, Copper sulphate solution with a constant concentration was prepared using $CuSO_4.5H_2O$ (10g/l) and H_2SO_4 (60 g/l). This concentration was obtained by adding 39.37g of $CuSO_4.5H_2O$ to about 700ml of distilled water. Then to this 31.7 ml of concentrated H_2SO_4 added and the distilled water was added again to make the solution up to 1 litre. The solution prepared attained a slightly high temperature due to the exothermic nature of the reaction. So the beaker containing the solution was kept in a freezer till the desired temperature was reached. Temperature was varied from 25°C to 5°C with an interval of 5°C. Acid concentration was varied from $20gl^{-1}$ to $40gl^{-1}$ and Copper concentration was varied

as $10gl^{-1}$ to $20gl^{-1}$ with an interval of 5 gl^{-1}. Electrolyte preparation for varying acid and copper concentration involved exactly similar steps but a calculated amount of $CuSO_4.5H_2O$ and H_2SO_4 was added. The parameters have been shown in Table 1.

Table 1. Electrolytic bath composition

Electrolyte composition for variation of Temperature		
Temperature (°C)	**Copper Sulphate ($CuSO_4.5H_2O$) (g)**	**Sulphuric Acid (H_2SO_4) (ml)**
5	39.37	31.7
10	39.37	31.7
15	39.37	31.7
20	39.37	31.7
25	39.37	31.7
Electrolyte composition for variation of Copper concentration		
Temperature (°C)	**Copper Sulphate ($CuSO_4.5H_2O$) (g)**	**Sulphuric Acid (H_2SO_4) (ml)**
25	**39.37**	31.7
25	**59.05**	31.7
25	**78.74**	31.7
Electrolyte composition for variation of Acid concentration		
Temperature (°C)	**Copper Sulphate ($CuSO_4.5H_2O$) (g)**	**Sulphuric Acid (H_2SO_4) (ml)**
25	39.37	**10.58**
25	39.37	**15.87**
25	39.37	**21.16**

3.4. Electrochemical cell and instrumentation

The experiments were done with ECOCHEMIE Autolab PGSTAT 12 potentiostat system and three electrode electrochemical cell. An Ag/AgCl and a Pt electrode were used as the counter and reference electrodes respectively. The graphite substrate was used as the working electrode. The operating parameters were variation in bath temperature, varying copper ion concentration and varying sulphuric acid concentration. The figure below shows a schematic diagram of the experimental setup.

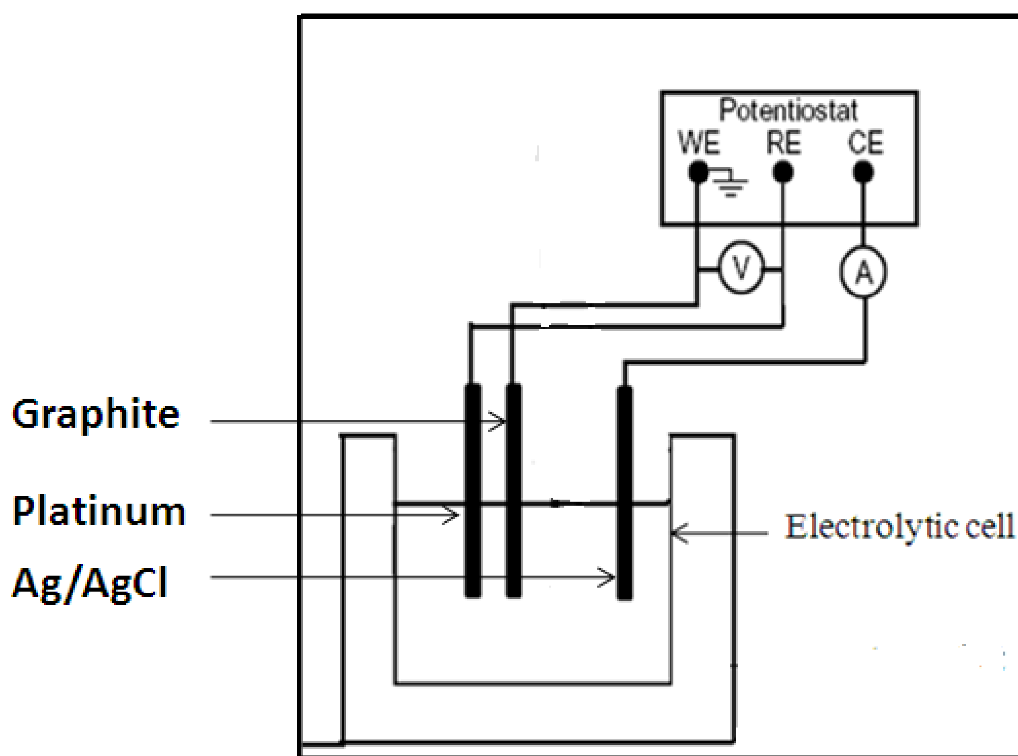

Fig. 7. Schematic diagram of the Electrochemical cell used

3.5. Cyclic voltammetry

In this technique, the input potential signal is a potential of a stationary working electrode is scanned linearly by means of potentiostat and the resulting current is monitored. The potential was scanned between – 0.6 V and 1.0 V at the rate of 10mV/s and a cyclic voltammogram was obtained for different temperatures.

3.6. Chronoamperometry

Chronoamperometry was performed next for each of the parameters mentioned above at potentials of – 0.15 V, – 0.20 V, – 0.25 V, – 0.30 V, – 0.35 V, – 0.40 V and – 0.45 V. after application of these step potentials current (i) was measured as a function of time. The current (i.e., electrons) flows to the working electrode (WE) in order to bring its potential to some desired value. A potentiostat with a 3-electrode cell provides the current via the auxiliary electrode (AE) to the WE while the potential is measured with respect to a reference electrode (RE).

3.7. Characterization techniques

A scanning electron microscope (SEM JEOL 6480 LV) equipped with an energy dispersive X-ray detector of Oxford data reference system were used for the morphological analysis of the copper deposited at different experimental conditions. X-ray diffraction was carried out, in the range of scanning angel 40-100° at a scanning rate 2° per minute, with CuKα radiation (λ=1.5406A0) using Philips X' PERT System X-Ray Diffractometer. The crystallite size is determined by measuring the Bragg peak width at half the maximum intensity and putting its value in Scherer's formula.

$$B(2\theta) = \frac{K\lambda}{L\cos\theta} \qquad (3.1)$$

The constant of proportionality, K (the Scherrer constant) depends on the how the width is determined, the shape of the crystal, and the size distribution.

K=0.94 for FWHM of spherical crystals with cubic symmetry. (K actually varies from 0.62 to 2.08). Average crystallite sizes of copper deposit were determined by the Williamson-Hall formula (As Scherrer equation is valid only for powders or loosely bound deposits but not for hard and adherent deposits) which is given by:

$$FW(S)\times\cos(\theta)=\frac{K\times\lambda}{Size}+4\times Strain\times\sin(\theta) \qquad (3.2)$$

CHAPTER –IV

Results and discussion

4. Results and discussion

4.1. Voltammetric study

Cyclic voltammetry was first employed to analyze the reaction kinetics of the deposition process at each of the temperatures mentioned. Fig.8. shows typical voltammograms obtained in solution at different temperatures. The parameters obtained from the cyclic voltammograms have been shown in the Table 2.

Table 2 Parameters obtained from the cyclic voltammograms of the graphite electrode in $CuSO_4$ solution at different temperatures (a) 5°C (b) 10°C (c) 15°C (d) 20°C and (e) 25°C.

Temp (°C)	I_C (A) (10^{-1})	E_C (V)	I_A (A) (10^{-1})	E_A (V)	Q^+ (C)	Q^- (C)	1st crossover potential (V)	2nd crossover potential (V)	$E_p - E_{p/2}$
5	-0.070	-0.434	0.078	0.199	1.280	-6.013	-0.368	-0.144	-0.002
10	-0.079	-0.453	0.073	0.237	1.544	-6.189	-0.367	-0.163	-0.042
15	-0.040	-0.432	0.133	0.293	2.792	-3.046	-0.353	-0.021	-0.037
20	-0.055	-0.391	0.242	0.330	4.893	-5.297	-0.249	0.013	-0.036
25	-0.049	-0.391	0.281	0.320	4.752	-4.989	-0.249	0.079	-0.028

In each voltammogram two peaks were obtained. Peak (I_c) is associated with Cu (II) reduction process (deposition) whereas peak (I_a) represents the Cu dissolution process from the graphite

electrode. The voltammograms were swept starting from 0 V to more negative direction up to – 0.6 V and then reversed at the same scan rate up to an anodic potential of 1.0 V.

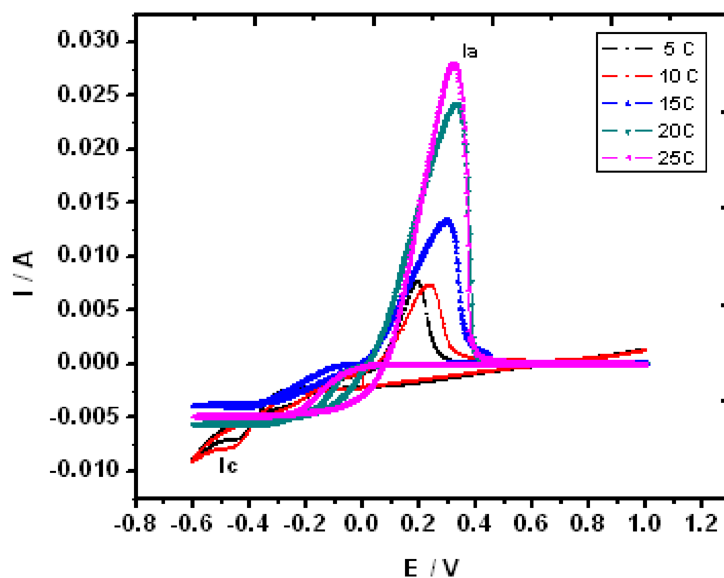

Fig.8. A set of cyclic voltammograms for the graphite electrode in $CuSO_4$ bath ($10gl^{-1}$ Cu^{2+} and $60gl^{-1}$ H_2SO_4) at a scan rate of 10 mV s^{-1} for different temperatures indicated

The cathodic current increases and reaches a maximum value at potential E_c (with value I*c*) indicating that a reduction (deposition) is taking place and then drops due to depletion of the Cu(II) ions from the surrounding electrolyte. During the reverse scan oxidation occurs and a peak current is observed at E_a (corresponding to a value, I_a). It is found that with increase in temperature the reduction (cathodic) potential decreases i.e. the peak values are shifted towards the positive axis. This may mean that with increase in temperature the deposition is feasible at lower potentials. The cathodic peak current (Ic) is directly proportional to the temperature. The main striking feature of the voltammograms is that the plot during the anodic part of the cycle crosses over the plot of the cathodic cycle. This point on the CV where the cathodic and anodic currents intersect is referred to as the crossover voltage. The presence of crossovers indicates the

presence of a 3D nucleation. It is also observed from Fig.8. that the current of the reversed scan was always larger than that of the forward scan. This may be because most of the reduced copper was available for dissolution into Cu (II) ions.

For more detailed characterization of the nucleation processes, Chronoamperometric analysis was done.

4.2.Chronoamperometric study

Chronoamperometric studies were performed with the same constant concentration as used for Voltammetric study. Different shapes of potentiostatic current transient curves were observed for different temperatures and potentials. Comparison is done by plotting the current transients at different potentials at a constant temperature and also vice versa i.e. by plotting them for different temperatures at a particular potential (Fig.9.).

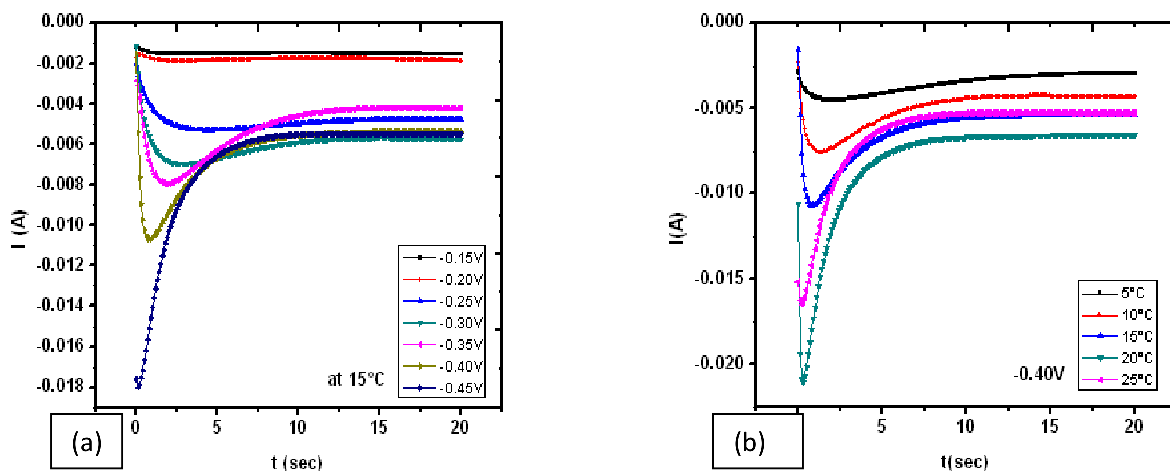

Fig.9. Current transients obtained for (a) a particular temperature 15°C at different potentials and (b) at different temperatures for a particular potential – 0.40 V

The current increases and reaches a maximum, and then decreases when the diffusion fields overlap. With increase in potential at a constant temperature we see that the current maxima

increases (in negative axes) indicating an increase in number of active sites of nucleation as well as the number of nuclei. Again with increase in temperature the current maxima are found to increase. This might indicate that the process is diffusion controlled as diffusion is temperature dependent.

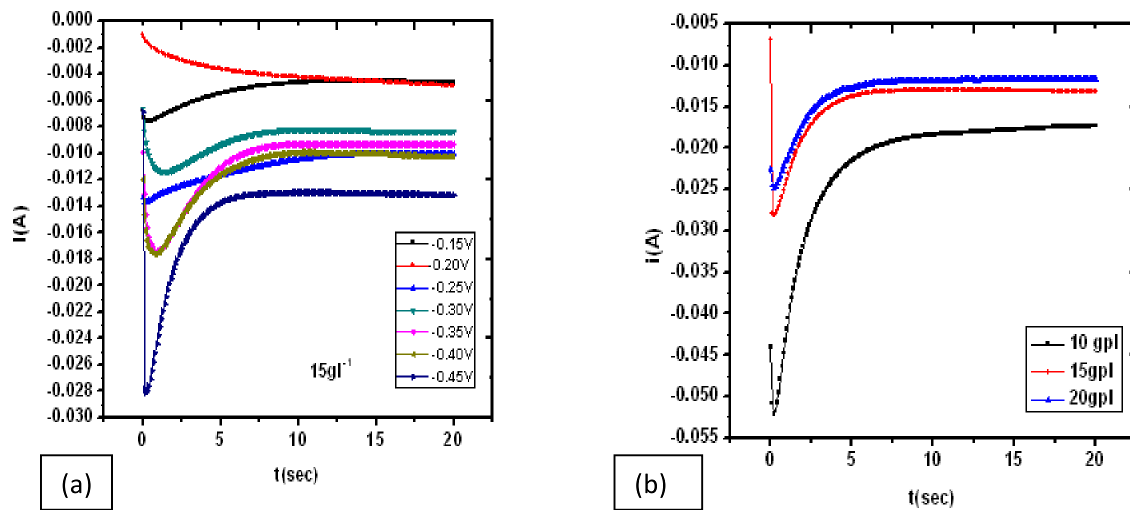

Fig.10. Current transients obtained for (a) a particular copper concentration 15gl^{-1} at different potentials (b) at – 0.45 V for copper concentrations of 10 gl^{-1}, 15 gl^{-1}, and 20 gl^{-1}

The current transients for deposition in varying copper concentrations have been shown in Fig.10. The maximum in the Cu ion reduction current, *Imax* (plotted in the figure as negative) increases in magnitude as the Cu concentration is stepped to increasing values.

.

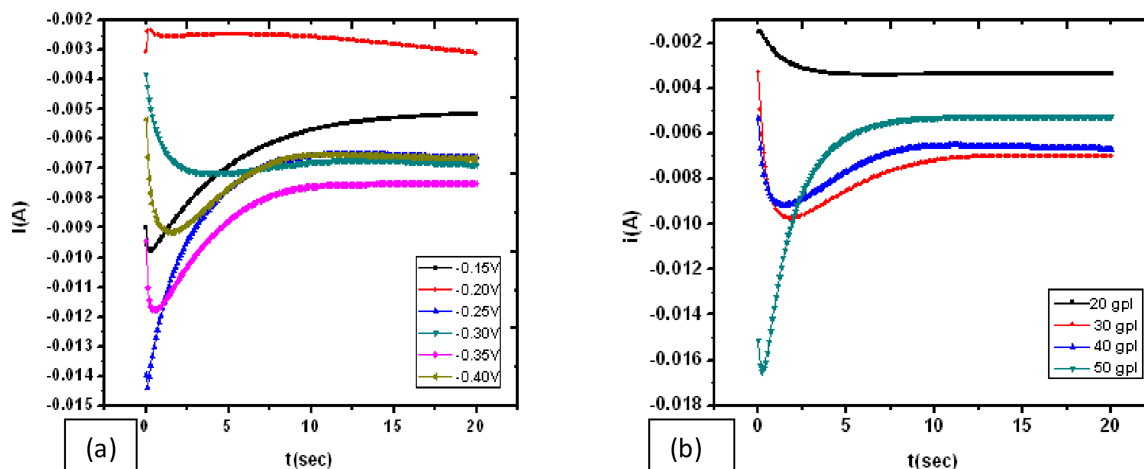

Fig.11. Current transients obtained for (a) a particular acid concentration of 40gl^{-1} at different potentials (b) – 0.40 V at acid concentrations of 20gl^{-1}, 30 gl^{-1}, and 40 gl^{-1}and 50 gl^{-1}

The varying acid concentration effect is shown in Fig.11. It can be clearly seen that the shape of the current transients changes as the acid concentration is stepped to increasingly more concentration values. With increase in acid concentration the magnitude of current increases.

4.3. Mathematical modeling

The theoretical formulations utilized for the description of the phase formation onto a substrate usually consider two extreme cases of nucleation: instantaneous and progressive. In instantaneous nucleation all nuclei form at the same time and grow comparatively slowly. In progressive nucleation new nuclei form during the course of deposition process and grow relatively faster [31]. In this paper we use theoretical non-dimensional curves of these extreme cases of nucleation for 2D or 3D growth. It helps us to define the dominant mechanism of the nucleation and growth for each of the studied temperature. The current transients obtained above are represented in dimensionless form and compared with theoretical transients.

4.3.1. 2D Model

The current transients were analyzed by the theoretical model proposed by Bewick et al. [32]. This model describes the kinetics of the electrolytic phase formation at the early stages of 2D growth. It takes into account two kinds of nucleation processes, instantaneous and progressive, which can be described by equations (4.1.) and (4.2) respectively.

$$\frac{j_{ins}}{j_m} = \frac{t}{t_m} \exp\left(\frac{-(t^2 - t_m^2)}{2t_m^2}\right) \qquad (4.1)$$

$$\frac{j_{pro}}{j_m} = \frac{t^2}{t_m^2} \exp\left(\frac{-2(t^3 - t_m^3)}{3t_m^3}\right) \qquad (4.2)$$

Where j is the current density, t is the time, ins and pro are referred to maximum in the transient to instantaneous and progressive nucleation respectively; m is referred to the maximum in the transient.

No fit was observed for any of the five temperatures. The current decays more slowly as compared to the theoretical curves. Fig.12. compares the experimental curve with the instantaneous and progressive curves calculated using equations (4.1) and (4.2). Clearly the growth of copper does not follow the 2D characteristics.

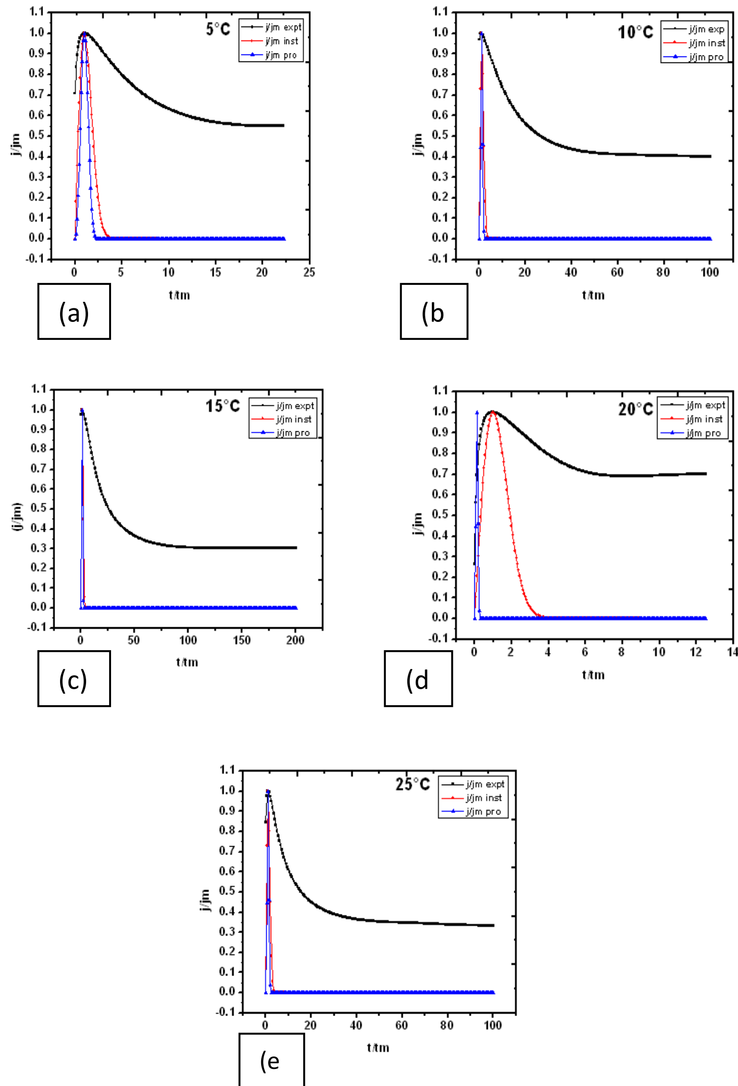

Fig.12. Dimensionless plots according to the equations (4.1) and (4.2) for two dimensional growth of copper deposits at (a) 5°C (b) 10°C (c) 15°C (d) 20°C (e) 25°C for a potential of – 0.45 V

The current transients for varying copper concentrations when compared with theoretical curves of Bewick model (Fig.13.) show that the experimental curve is nowhere close to either of the two curves, i.e., instantaneous or progressive. So, copper deposition does not follow 2D growth characteristics.

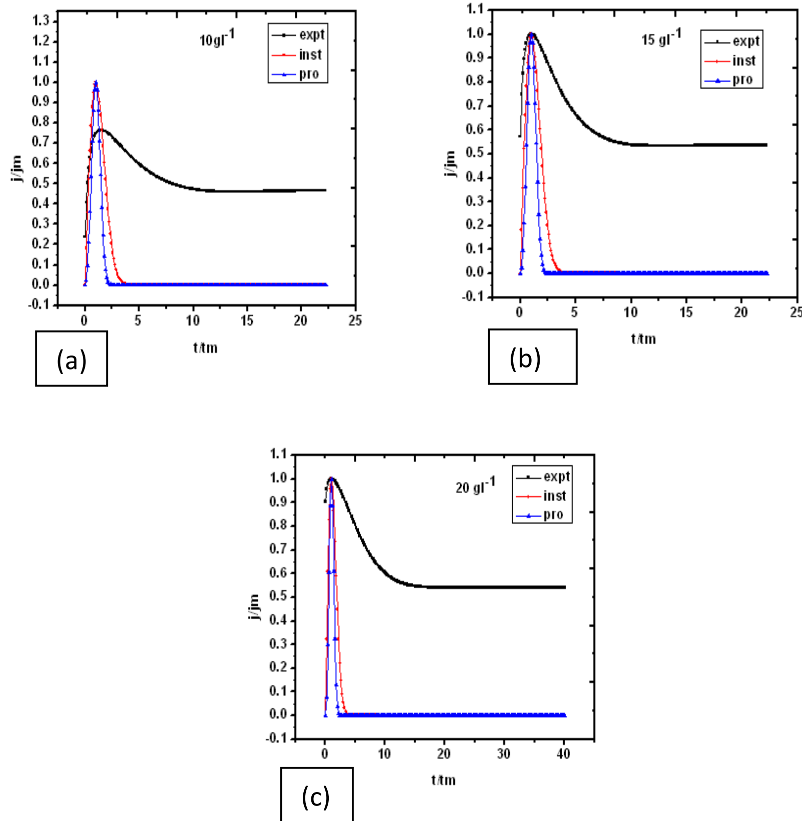

Fig.13. Dimensionless plots according to equations (4.1) and (4.2) for two dimensional growth of copper deposits at Copper concentrations of (a) 10gpl (b) 15 gpl and (c) 20gpl at a potential of –0.35 V

No fit was observed for any of the plot at three different acid concentrations. The current decays more slowly as compared to the theoretical curves. Fig.14. compares the experimental curve with the instantaneous and progressive curves calculated using equations (1) and (2). Clearly the growth of copper does not follow the 2D characteristics.

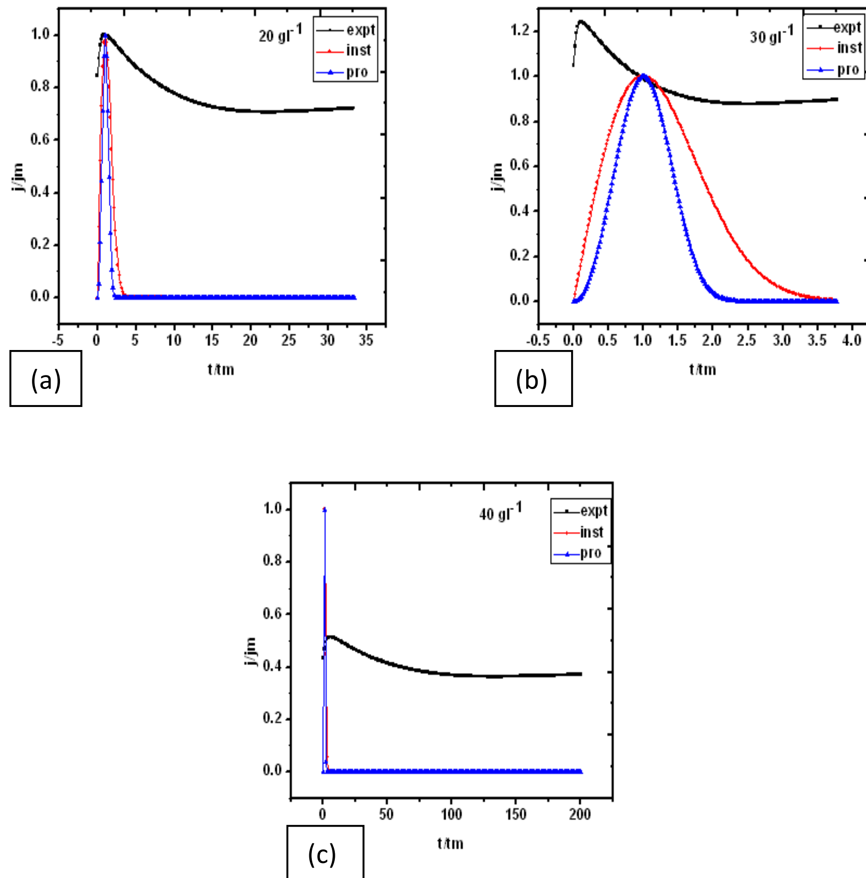

Fig.14. Dimensionless plots according to the equations (4.2) and (4.3) for two dimensional growth of copper deposits at varying acid concentrations of (a) 20gpl (b) 30 gpl and (c) 40 gpl at a potential of –0.25 V

4.3.2. 3D Model

The models proposed by Scharifkar and Hills [33] describe phase formation at early stages when diffusion of the electro active species from the bulk to interface is the slowest step of the whole process. According to the model the instantaneous and progressive type nucleation are described by equations (4.3) and (4.4)

$$\frac{I^2}{I_m^2}(instantaneous) = \frac{1.9542}{\frac{t}{t_m}}\{1 - \exp[-1.2564(\frac{t}{t_m})]\}^2 \quad (4.3)$$

$$\frac{I^2}{I_m^2}(progressive) = \frac{1.2254}{\frac{t}{t_m}}\{1-\exp[-2.3367\left(\frac{t}{t_m}\right)^2]\}^2 \qquad (4.4)$$

The values $(i/i_m)^2$ were plotted against t/t_m. Fig.15. compares the experimental results with the two limiting cases of theoretical three dimensional nucleation growth models at a constant potential of – 0.45 V for different temperatures.

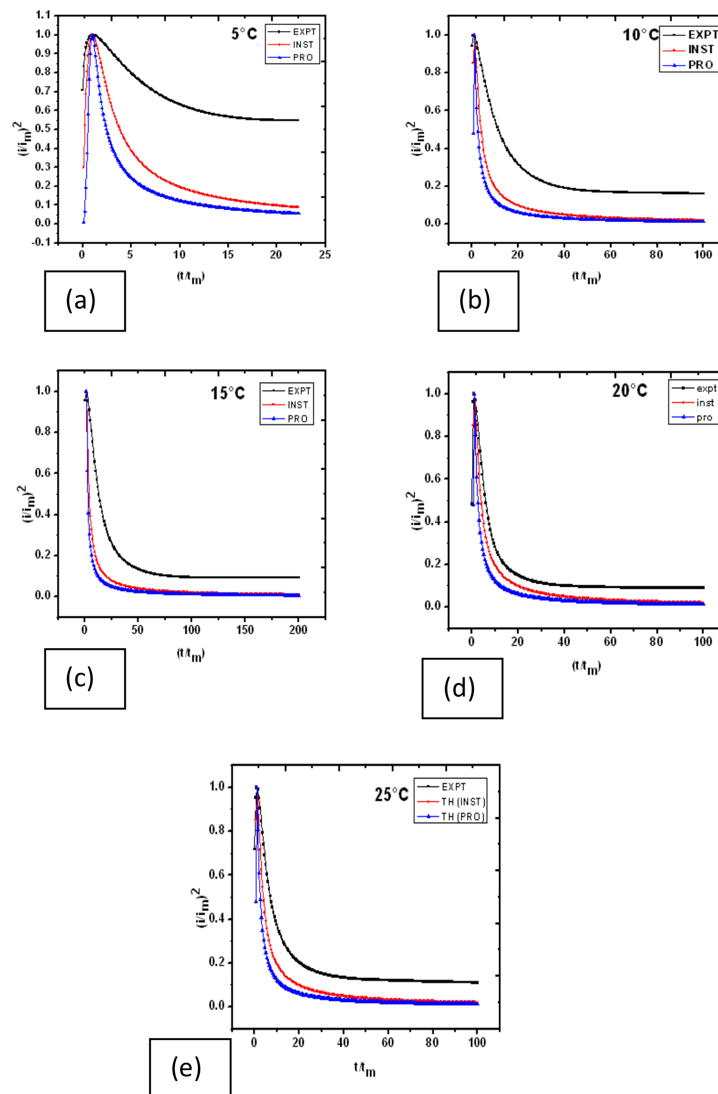

Fig.15. Dimensionless plots according to the equations (4.3) and (4.4) for three dimensional growth of copper deposits at (a) 5°C (b) 10°C (c) 15°C (d) 20°C (e) 25°C

The results suggest that the nucleation increasingly becomes closer to instantaneous at higher temperatures

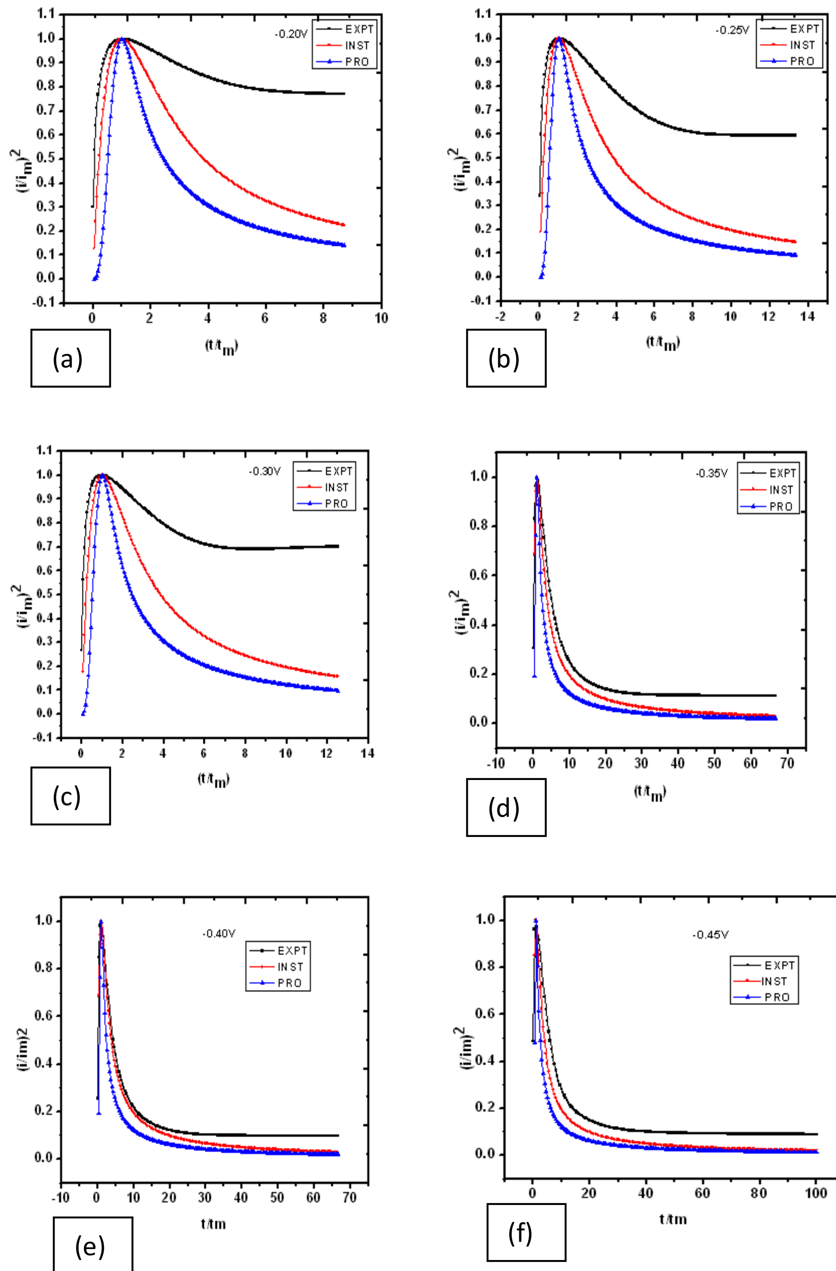

Fig.16. Dimensionless plots according to the equations (4.3) and (4.4) for three dimensional growth of copper deposits at 20 °C for increasing potentials of (a)– 0.20 V, (b)– 0.25 V, (c)– 0.30 V,(d) – 0.35 V, (e)– 0.40 V and (f)– 0.45 V

Similarly, Fig.16 compares the experimental curves at a constant temperature (20°C) for different applied potentials. No fit was observed for lower potentials. However, the curves follow the three dimensional instantaneous growth model at higher potentials for the same temperature.

The Fig.17 shows the current transients, obtained from variation of copper concentration, fitted into the 3D SH model. It is seen that at lower concentrations (10 gl^{-1}) of copper the experimental curve completely coincides with the theoretical curve for instantaneous nucleation. However when copper concentration is increased the experimental curve deviates from the theoretical curves. So we can conclude that copper deposition undergoes instantaneous nucleation at lower concentrations.

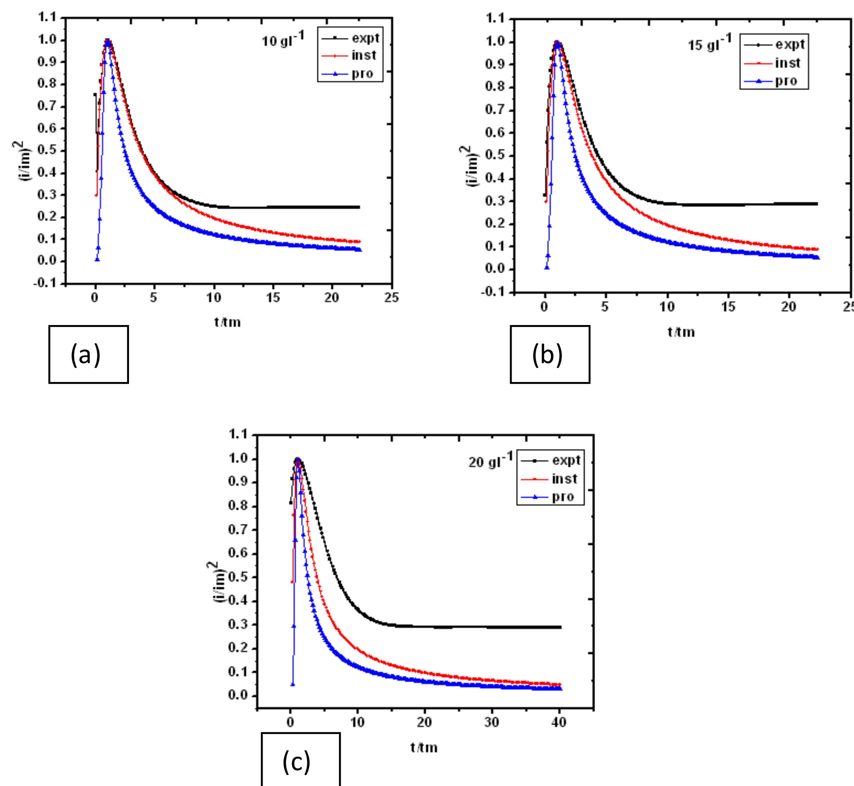

Fig.17. Dimensionless plots according to the equations (4.3) and (4.4) for three dimensional growth of copper deposits at varying copper concentrations of (a)10 gl^{-1} (b)15 gl^{-1} (c) 20 gl^{-1}

Fig.18. compares experimental results of acid concentration variation with the theoretical curves proposed by SH model. It is seen that the nucleation part of the curve completely overlaps with the theoretical curve obtained for instantaneous nucleation while the growth behaviour does not match. So we can say that copper deposition follows instantaneous nucleation. The deposition might follow a mixed (both 2D and 3D) growth mode.

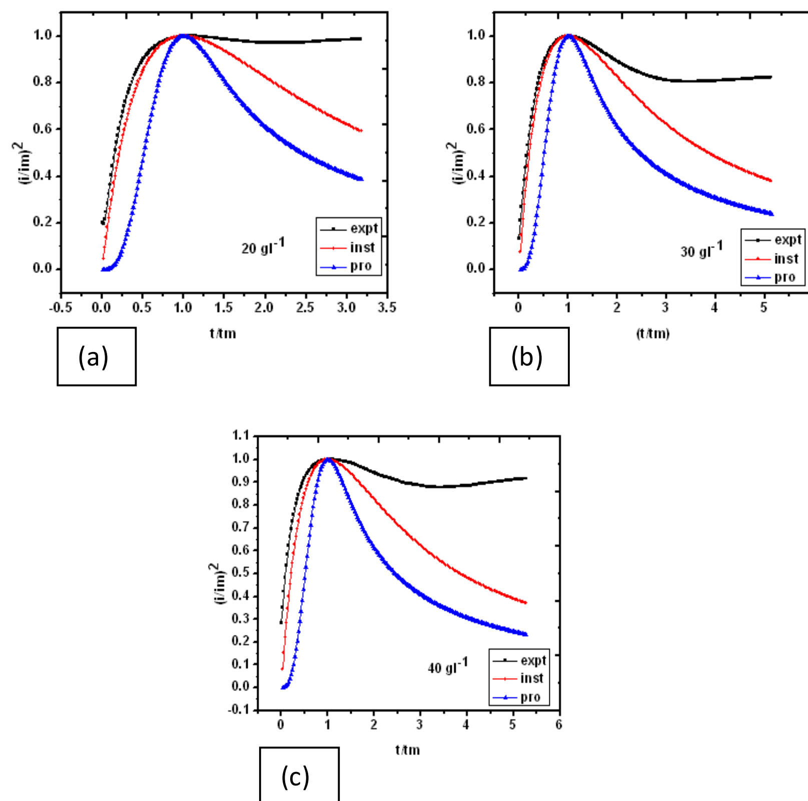

Fig.18. Dimensionless plots according to the equations (4.3) and (4.4) for three dimensional growth of copper deposits at varying acid concentrations of (a)20 gl^{-1} (b)30 gl^{-1} (c) 40 gl^{-1}

4.4. Phase and structural analysis

Fig.19. shows the SEM analysis of the samples at various temperatures at – 0.35 V

The figure shows the topographies of the graphite electrodes modified at different temperatures. From a fixed solution a clear change in the morphology, density of Cu nuclei and surface

transition of dendritic structures to non-dendritic and spherical grain morphology with reduction in bath temperature.

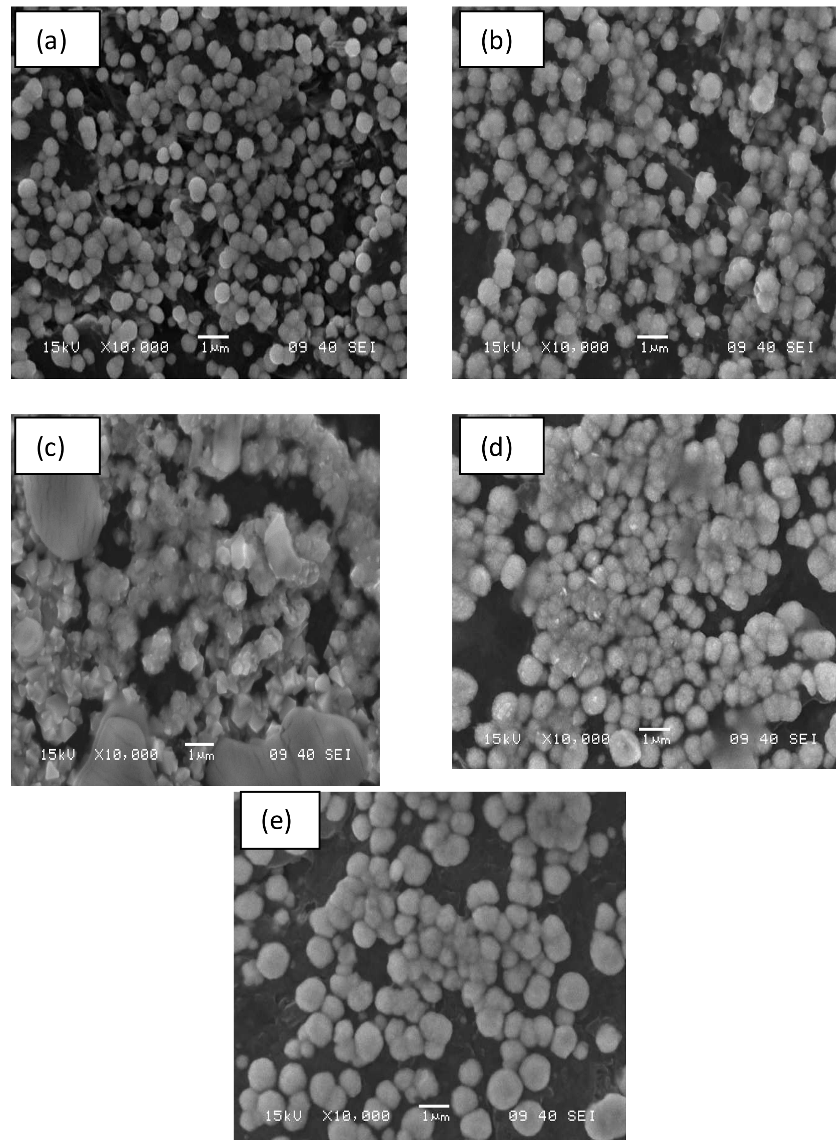

Fig.19. SEM images of copper deposits at (a)5°C, (b)10°C, (c)15°C, (d)20°C and (e)25°C

This morphological transition can be an indication of changeover of a muddled system to a more stable one. Indeed, an increase in both the number of nuclei and surface coverage is observed upon shifting the temperature from 25 °C to 5 °C. For the former, the Cu deposit covers about 30% of the surface and for low temperature depositions the coverage has increased remarkably.

The increase in nuclei population density at low synthesizing temperatures allows an early overlapping of spherical diffusion zones. The eventual overlap will inhibit the total amount of material available for further growth of the supercritical nuclei. This in turn might have resulted fine copper spheroids in deposits electroplated at reducing bath temperatures.

On varying the copper concentration at constant acid concentration and temperature it was observed that the surface coverage of the deposits increases as the copper concentrate in the bath is increased (Fig.20.). There is formation of non-dendritic and spherical grain morphology with change in copper concentration.

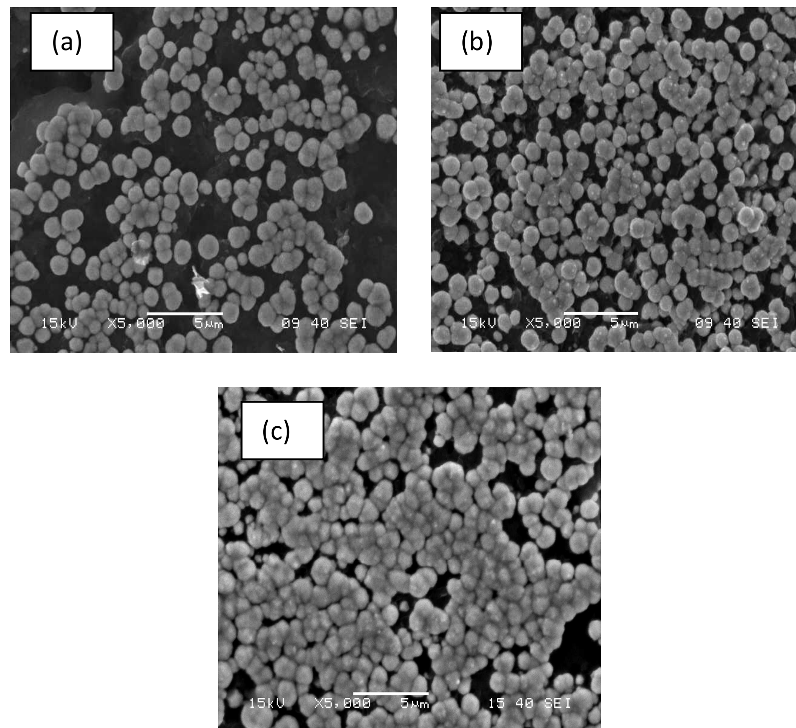

Fig.20. SEM images of copper deposits at varying copper concentrations of (a)10 gl^{-1}, (b) 15gl^{-1} (c) 20 gl^{-1}

The Fig.21 below shows the SEM analysis of the samples at varying acid concentrations. It was found that acid concentration strongly affects the density of Cu nuclei, their size and the surface

coverage. With the increase in acid concentration there is vigorous evolution of hydrogen resulting in a porous structure at higher acid concentrations. Also there is tendency for agglomeration at higher acid concentrations.

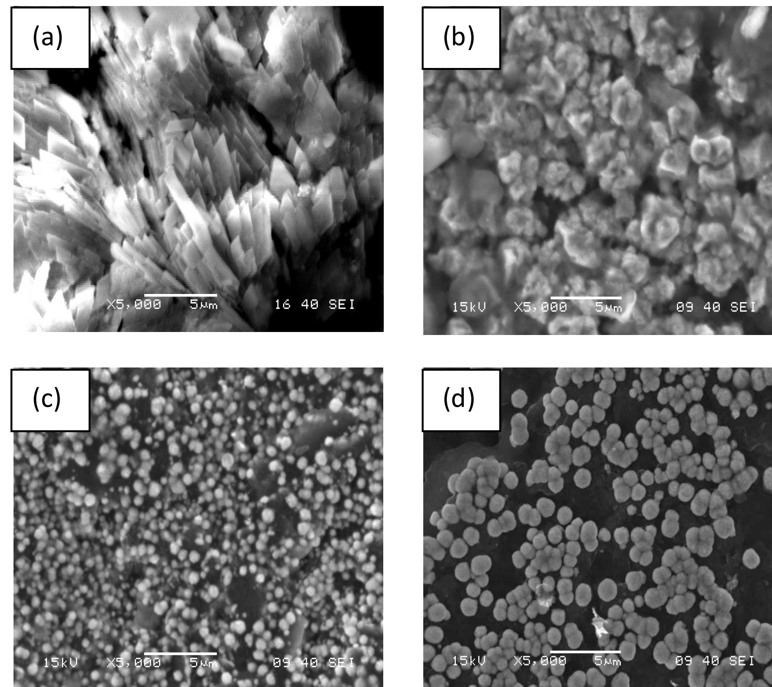

Fig.21. SEM images of copper deposits at varying acid concentrations(a) 20 gl^{-1}, (b) 30gl^{-1}, (c) 40 gl^{-1} and (d) 50 gl^{-1}

Fig.22. represents the XRD pattern of copper deposits at various bath (a) temperatures, (b) copper concentration and (c) acid concentration. The diffraction peaks at 2θ = 43.317 can be indexed as the [111] plane of copper. The peaks show high crystallinity of copper with some carbon peaks because of the substrate. It was however found that the copper was deposited only on the [111] plane indicating a highly textured deposit.

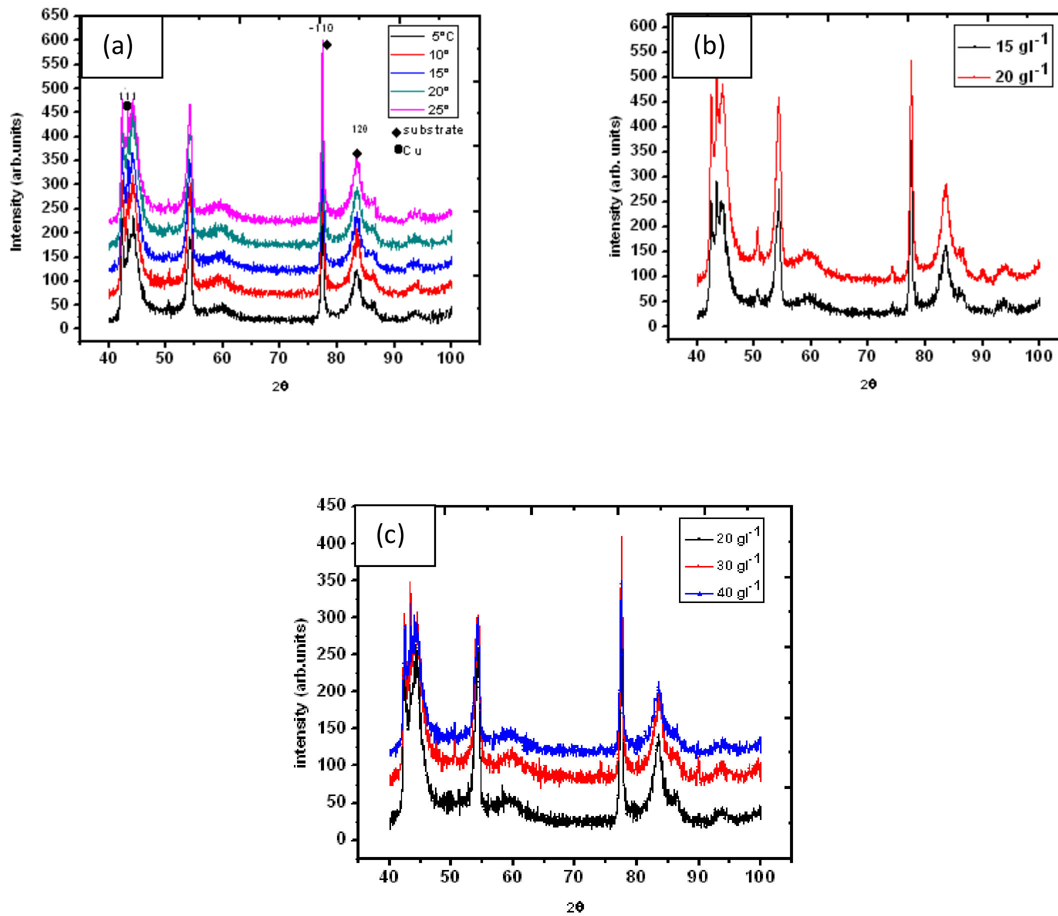

Fig.22. XRD patterns for the Cu films deposited at varying (a) temperatures (b) copper concentrations and (c) Acid concentrations

With decreasing temperature, broadening increases where as intensity decreases and with increasing acid and copper concentration intensity is found to increase. The broadening of peaks can be attributed to small particle size and strain of crystalline materials. Table 3 shows the crystallite size and lattice strain obtained by varying different parameters.

Table 3. Crystallite size and lattice strain obtained by varying different parameters

With variation in temperature			
Potential (V)	**Temperature (°C)**	**Crystallite size (nm)**	**Lattice strain (%)**
– **0.35 V**	5	37.5	25.2
– **0.35 V**	10	41.3	23.0
– **0.35 V**	15	46.0	20.5
– **0.35 V**	20	51.0	15.6
– **0.35 V**	25	147.4	6.6
With variation in copper concentration			
Potential (V)	**Copper concentration (gl^{-1})**	**Crystallite size (nm)**	**Lattice strain (%)**
– **0.45 V**	15	39.2	24.2
– **0.45 V**	20	66.8	14.3
With variation in acid concentration			
Potential (V)	**Acid concentration (gl^{-1})**	**Crystallite size (nm)**	**Lattice strain (%)**
– **0.45 V**	20	46.7	17.6
– **0.45 V**	30	45.5	20.8
– **0.45 V**	40	39.2	24.2

CHAPTER –V
Conclusion

5. Conclusion.

Copper films were deposited on a graphite substrate from a simple aqueous solution containing $CuSO_4.5H_2O$ and H_2SO_4 with varying electrolyte temperature, metal ion concentration and the acid concentration. The results obtained from the above studies have been summarized here.

While studying the reaction and nucleation mechanism of copper, it was found that copper nucleates according to 3D instantaneous nucleation mechanisms for all the parameters. The extent of nucleation was found to increase at low temperatures. There was also increase in surface coverage and nuclei density. On increasing metal ion concentration a tendency toward agglomeration and coarser grain formation was observed. Finer grains were produced on increasing acid ion concentration. This was further confirmed by XRD analysis.

Thin film has already revolutionized material development and their applications in a wide and critical field. Hence, the present research may direct further emphasis on investigation and production of ultra fine grained (in nano range) thin films.

6. References

[1] SreeHarsha K.S., Principles of Physical Vapor Deposition of Thin Films, UK: Elsevier Ltd., 2006

[2] Mallik A., Effects of temperature and ultrasound on nucleation behaviour during electrochemical synthesis of copper thin films, PhD thesis, National Institute of Technology, Rourkela, 2010

[3] Horowitz F., Pereira M., and Azambuja G. de., Glass window coatings for sunlight heat reflection and co-utilization, Appl. Opt., 50 (2011), pp. C250-C252

[4] Chopra K.L., Kaur I. Thin Film Device Application, New York & London: Plenum Press, 1983

[5] Adhihetty Indira S., Vella Joseph B., et al. Mechanical properties, adhesion, and fracture toughness of low-k dielectric thin films for microelectronic applications, Mat. Res. Soc, 716 (2002), B12.13.1-13.6

[6] Mahan John E. Physical Vapor Deposition of Thin Films, New York: Americal vacume society, John-Wiley and Sons, 2000

[7] Thin film, http://en.wikipedia.org/wiki/Thin_film/07.05.2011]

[8] Eskhult J., Electrochemical deposition of nanostructured metal/metal oxide coatings, Doctoral dissertation, Acta Universitatis Upsaliensis Uppsala, 2007

[9] Bankoti A. K. S., Synergistic study of electrochemically deposited thin film with a spectrum from micro to nano range structures, M-Tech thesis, National Institute of Technology, Rourkela, 2009

[10] Bicelli L. P., Bozzini B., Mele C., D'Urzo L., A review of nanostructured aspects of metal electrodeposition; International Journal of Electrochemical Science, 3 (2008), pp 356-408

[11] Paunovic M., Schlesinger M., Fundamentals of Electrochemical Deposition, USA: Wiley Interscience, 2006

[12] Bard J., Faulkner L. R., Electrochemical methods: Fundamentals and applications, USA : John Wiley and Sons, 2001

[13] Yoreo James J. D, Vekilov Peter.G. Principles of crystal nucleation and growth, Reviews in Mineralogy and Geochemistry, 54 (2003), pp. 57-93

[14] Raghavan V., Physical Metallurgy, Principles and Practice, New Delhi: Prentice Hall of India Private Ltd., 2006

[15] Singh V. Physical Metallurgy, Standard Publishers & Distributors, 2005

[16] Zainal Z., Kassim A., Hussain M.Z., Ching C. Effect of bath temperature on the electrodeposition of copper tin selenide films from aqueous solution, 58 (2004), pp. 2199-2202

[17] Ramı´rez Claudia, Arce Elsa M., Romero-Romo Mario, et al. The effect of temperature on the kinetics and mechanism of silver electrodeposition, Solid State Ionics 169 (2004), pp. 81-85

[18] Dulal S.M.S.I., Hyeong Jin Yun, Chee Burm Shin, et al. Electrodeposition of CoWP film III. Effect of pH and temperature, Electrochimica Acta, 53 (2007), pp. 934–943

[19] Cheng S., Chen G. Chen Y., Huang C, Effect of deposition potential and bath temperature on the electrodeposition of SnS film, Thin solid film, I 29 (2006), pp. 439-444

[20] Fenineche N. and Coddet C. Effect of electrodeposition parameters on the microstructure and mechanical properties of Co-Ni alloys; Surface Coating Technology, 41 (1990), pp. 75-81

[21] Radovici O, Vass C., and Solacolu I. Some aspects of copper electrodeposition from pyrophosphate electrolytes; Electrodeposition and Surface treatment, 2 (1973/74), pp. 263-273

[22] Seo M. H., Kim D. J., Kim J. S.; The effect of pH and temperature on Ni-Co-P alloy electrodeposition from a sulphate bath and the material properties of the deposits; Thin Solid Films, 489 (2005), pp. 122-129

[23] Mahalingam T., Raja M., Thanikaikarasan S., Sanjeeviraja C., et al., Electrochemical deposition and characterization of Ni-P alloy thin films; Materials Characterization, 58 (2007), pp. 800-804

[24] Schlesinger M., Paunovic M., Modern Electroplating, New York: Wiley, 2000

[25] Finch, G. I. and Wilman, H. and Yang, L, Crystal growth at the cathode, Discuss. Faraday Soc., 1 (1947), pp. 144-158

[26] Setty T.H.V. and Wilman H., Crystal growth at the cathode, Trans.Faraday Soc., 51 (1955), pp. 984

[27] Pangarov N. A., Rashkov S., Compt. Rend. Acad. Bulgare Sci., 13 (1960), pp. 555

[28] Pangarov N. A., Rashkov S., Compt. Rend. Acad. Bulgare Sci., 13 (1960), pp. 439

[29] Fleischmann M., Thirsk H. R., Trans. Faraday Soc., 51 (1955), pp. 71

[30] Hyde M. E., Compton R. G., A review of the analysis of multiple nucleations with diffusion controlled growth, J. Electroanal. Chem., 549 (2003), pp. 1-12

[31] Majidi M.R, Asadpour-Zeynoli K, Hafezi B,; Reaction and Nucleation mechanisms of copper electrodeposition on disposable pencil graphite electrode; Electrochimica Acta, 54 (2009), pp 1119-1126

[32] Bewick A., Fleischmann M., Thirsk H.R., Kinetics of Electrocrystallisation of Thin Films of Calomel, Trans Faraday Soc., 58 (1962), pp. 2200

[33] Scharifker B. and Hills B., Theoretical and experimental studies of multiple nucleation, Electrochimica Acta., 28 (1982), pp. 879-889